Geometric, electronic, and optical properties of the Si(111)2×1 surface: Positive and negative buckling

C. Violante,[1] A. Mosca Conte,[1] F. Bechstedt,[2] and O. Pulci[1,3]

[1]*ETSF, MIFP, Dipartimento di Fisica, Università di Roma Tor Vergata, Via della Ricerca Scientifica 1, I-00133 Rome, Italy*

[2]*ETSF, IFTO, Friedrich-Schiller-Universität, Max-Wien-Platz 1, 07743 Jena, Germany*

[3]*Istituto di Struttura della Materia, Consiglio Nazionale delle Ricerche, Via del Fosso del Cavaliere 100, I-00133 Rome, Italy*

(Received 8 August 2012; revised manuscript received 25 October 2012; published 14 December 2012)

The Si(111)2×1 is among the most investigated surfaces. Nonetheless, several issues are still not understood. Its reconstruction is well explained in terms of the Pandey model with a slight buckling (tilting) of the topmost atoms; two different isomers of the surface, conventionally named positive and negative buckling, exist. Usually, scanning tunneling microscopy (STM) experiments identify the positive buckling isomer as the stable reconstruction at room temperature. However, at low temperatures and for high *n* doping of the substrate, recent scanning tunneling spectroscopy (STS) measurements found the coexistence of positive and negative buckling on the Si(111)2×1 surface. In this work, state-of-the-art *ab initio* methods, based on density functional theory and on many-body perturbation theory, have been used to obtain structural, electronic, and optical properties of Si(111)2×1 positive and negative buckling. The theoretical reflectance anisotropy spectra (RAS), with the inclusion of the excitonic effects, can provide a way to deepen the understanding of the coexistence of the isomers.

DOI: 10.1103/PhysRevB.86.245313 PACS number(s): 71.15.Nc, 78.68.+m, 71.35.−y, 78.40.−q

I. INTRODUCTION

The Si(111)2×1 surface is one of the most studied and well-known reconstructed semiconductor surfaces. The (111) planes are the natural cleavage surfaces of the elemental semiconductors and the 2×1 reconstruction is the one observed for Si samples after cleavage in ultrahigh vacuum at low temperature. The atomic structure of Si(111)2×1 consists of zigzag chains of π-bonded atoms along the $[1\bar{1}0]$ direction, well described within the Pandey model.[1] Pseudopotential total-energy calculations have shown that this reconstruction can be formed easily in the cleavage process.[2] In order to describe properly all the experimental data, a buckling (i.e., a tilting) of the atoms of the chains has to be considered. Moreover, *ab initio* calculations have shown that the buckled structure is energetically more stable.[3] Two different ways of tilting the topmost atoms of the Pandey chains exist, giving rise to two isomers of Si(111)2×1.[3] They differ for the conventional sign of the buckling: The Si(111)2×1 positive buckling (pb) and the Si(111)2×1 negative buckling (nb) (see Figs. 1 and 2).

Si(111)2×1 positive and negative buckling are inequivalent structures with respect to the third atomic layer: This little difference in the surface geometry gives rise to significant differences in the electronic and optical properties, as shown in this work. Scanning tunneling microscopy (STM) measurements[4] suggest that in standard conditions (low doping and room temperature) the Si(111)2×1 positive buckling is the most stable atomic structure. Nonetheless, a recent work[5] on highly *n*-doped specimens of Si(111)2×1 has shown, comparing data from scanning tunneling spectroscopy (STS) measurements and theoretical predictions, the coexistence of both isomers of the surface at very low temperature (8 K). This coexistence, for which the level of doping is a crucial parameter,[6] has also been proved at room temperature.[7] Therefore, a deeper study of the Si(111)2×1 negative buckling is needed. The study of the surface optical properties can provide the definitive proof of the coexistence and insight into the electronic structure of the two isomers. A combined effort of theoretical simulations and experimental data concerning optical spectra is often a powerful tool to confirm or discard a particular surface model.[8,9] The inclusion of the electron-hole interaction in the theoretical optical spectra of surfaces is a major issue: The excitons within the electronic gap (bound electron-hole states) cannot be neglected in order to reproduce experimental results. In this work we compute the geometric, electronic, and optical properties of both isomers of Si(111)2×1 by *ab initio* calculations among the most reliable state-of-the-art methods based on density functional theory and many-body perturbative techniques (GW and Bethe-Salpeter equation). The differences between the two isomers concerning the quasi-one-dimensional surface excitons determine a different optical response of the two surfaces.

II. METHODS

In order to model the Si(111)2×1 positive and negative buckling surfaces the supercell method was applied: We have used slabs of 24 atoms, forming 12 atomic layers, separated by 7.42 Å of vacuum for structural and energetic properties and by 17.12 Å of vacuum for electronic and optical properties. Tests with thicker slabs (up to 24 layers) have also been performed.

As a first step the geometric, electronic, and optical properties of both isomers of Si(111)2×1, positive buckling (pb) and negative buckling (nb), were calculated within the density functional theory (DFT) in the local density approximation (LDA), using the codes of the *Quantum Espresso* package.[10] We have employed a norm-conserving LDA pseudopotential and an exchange-correlation potential parametrized by Perdew and Zunger.[11,12]

We have sampled the Brillouin zone using Monkhorst and Pack uniform grids of (nk_1, nk_2, nk_3) k points[13] with (0,0,0) offset (not shifted k points) and (1,1,1) offset (shifted k points); offset 1 along a particular axis means a grid displaced by half a grid step in that axis. The number and the type of used k points are crucial parameters, as highlighted in the next section.

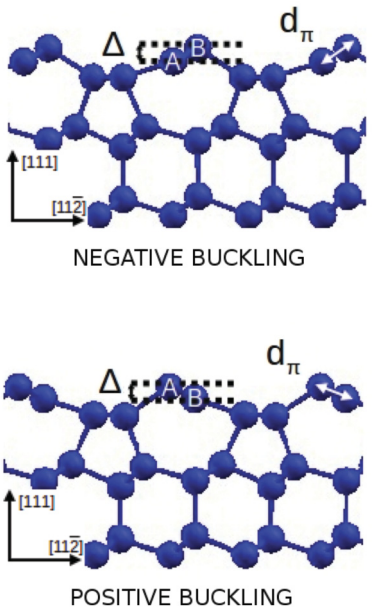

FIG. 1. (Color online) Side view of both isomers of Si(111)2×1. The distance d_π between atom A and atom B is the bond length along the Pandey chain, while the difference in height Δ between atom A and atom B is the buckling amplitude.

Quasiparticle energies have been calculated within the many-body perturbation theory in the GW approximation.[14] The electron-hole interaction has been taken into account by solving the Bethe-Salpeter equation[15](BSE). The inclusion of excitonic effects is often essential to describe properly the optical properties of the matter and to obtain theoretical results in good agreement (quantitative and qualitative) with experiments. In order to ease the computational applicability, the Bethe-Salpeter equation is rewritten as an eigenvalue problem involving the so-called "excitonic Hamiltonian" whose elements can be calculated starting from DFT wave functions, GW quasiparticle energies, and the screened Coulomb interaction W. BSE calculations have been carried out using the EXC code.[16]

Concerning the optical properties, we have focused on the reflectance anisotropy spectroscopy (RAS) spectra. RAS experiments[17,18] are a powerful and efficient tool widely used to study and characterize surfaces. The RAS signal measures the difference of reflectivity for light polarized along two perpendicular directions (x and y) in the plane of the surface:

$$\frac{\Delta R}{R} = \frac{R_y - R_x}{R}$$

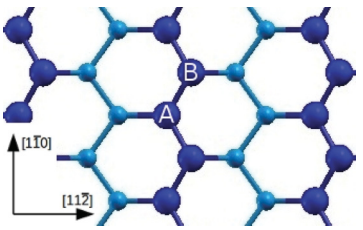

FIG. 2. (Color online) Top view of both isomers of Si(111)2×1.

and it corresponds to the difference of the reflectivity corrections to the Fresnel case for the two different light polarizations. For cubic crystals, the RAS signal comes from the surface anisotropy since the bulk is optically isotropic. The reflectance anisotropy spectroscopy is very suitable and widely used to combine experimental and theoretical effort; in fact, there is a simple expression for the RAS spectrum, in the case of the supercell method, involving the half-slab polarizability[19] $\alpha_{ii}^{\rm hs}$, related to the surface optical properties, and involving the bulk dielectric function ϵ_b, related to the volume (bulk) optical properties:

$$\frac{\Delta R_i}{R} = \frac{4\omega d}{c} \mathrm{Im} \frac{4\pi \alpha_{ii}^{\rm hs}}{\epsilon_b - 1},$$

where d is the half-slab thickness and i is the direction of light polarization.

The half-slab polarizability $\alpha_{ii}^{\rm hs}$ and the bulk dielectric function ϵ_b have been calculated within RPA using DFT-LDA and within the GW plus Bethe-Salpeter equation method.

In our choice, y is along the [1$\bar{1}$0] direction (parallel to the Pandey chains) and x is along the [11$\bar{2}$] direction (perpendicular to the Pandey chains).

III. RESULTS

A. Geometry and ground-state properties

As a consequence of minimization of total energy we have obtained the ground-state geometry of both isomers of Si(111)2×1 within DFT-LDA. With a cut-off energy of 30 Ry and a mesh of 100 shifted k points in the irreducible Brillouin zone (IBZ) we have determined the buckling amplitude Δ and the bond length d_π along the Pandey chains for the two different structures of the surface (see Fig. 1). Concerning the buckling amplitude, we have obtained

$$\Delta^{\rm pb} = +0.53 \text{ Å}, \quad \text{for the positive buckling},$$
$$\Delta^{\rm nb} = -0.59 \text{ Å}, \quad \text{for the negative buckling}.$$

Comparing with the most recent DFT calculations (2011), we find the same values as reported by Bussetti *et al.*[5] but also a good agreement with the hybrid DFT results by Patterson *et al.*[20] We also find good agreement with previous theoretical results.[4,21–23]

For the bond length along the Pandey chains, we have obtained $d_\pi = 2.27$ Å for both isomers. The bond distance along the π chains is contracted with respect to the bond length of the Si bulk ($d_b = 2.34$ Å in our calculations). Moreover, the absolute value $|\Delta|$ of the buckling amplitude of both isomers satisfies the relationship $|\Delta| = (0.2\text{–}0.3)d_b$, as reported by Bechstedt.[24] We find an excellent agreement between our prediction of the bond length and the LEED data by Xu *et al.*[25] ($d_\pi = 2.271$ Å) and a good agreement between the LEED data ($|\Delta| = 0.51$ Å) of the same authors and our calculated buckling amplitude for the pb isomer.

We have checked the convergence of the geometric values against the number of k points used to sample the IBZ: The increasing trend till convergence of the buckling amplitude for both isomers is shown in Fig. 3.

Si(111)2×1 negative and positive buckling are both local energy minima, separated by an energetic barrier as shown in

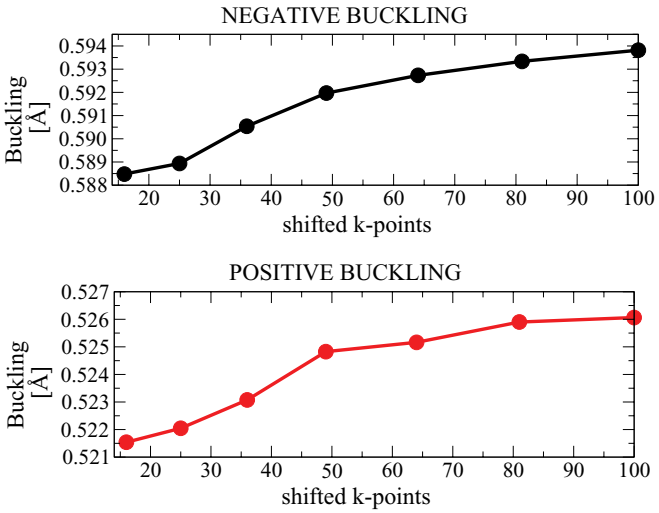

FIG. 3. (Color online) Buckling amplitude versus the number of k points used to sample the IBZ.

Fig. 4. We have estimated the upper limit value of the energetic barrier and we have found it to be about 0.06 eV/(2×1); the estimate has been done switching from the negative buckling configuration to the positive buckling one simply tilting "by hand" the buckled atoms of the Pandey chain with respect to each other. At each step, the system has been relaxed keeping fixed the value of the buckling amplitude.

Our calculations show that the negative buckling is the most stable configuration, being favored by about 5.4 meV/(2×1) compared to the positive buckling. There are contrasting results in the literature concerning this issue of the stability.[3,26] We suggest that the choice of the number and the type (quality) of the k points used to sample the Brillouin zone is crucial to establish which configuration is the stable one. The trend of DFT total energy against the number and the type of k points for both isomers is shown in Fig. 5.

We can notice that using not shifted k points (that is, a mesh of k points containing Γ and other k points on the border of the Brillouin zone) and increasing their number, there is an inversion of stability [see Fig. 5(b)]. Instead,

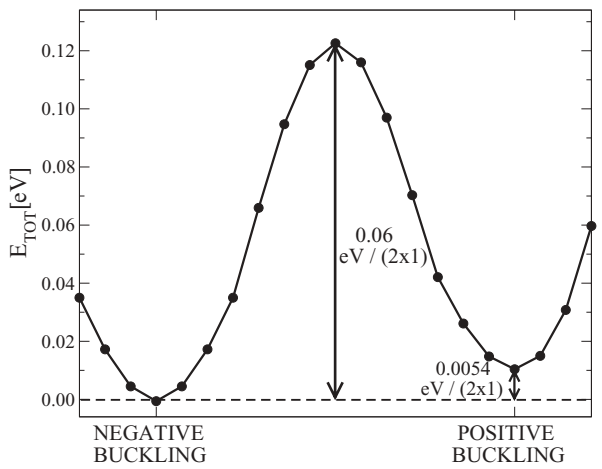

FIG. 4. Energy path from the negative buckling structure to the positive buckling configuration (see text).

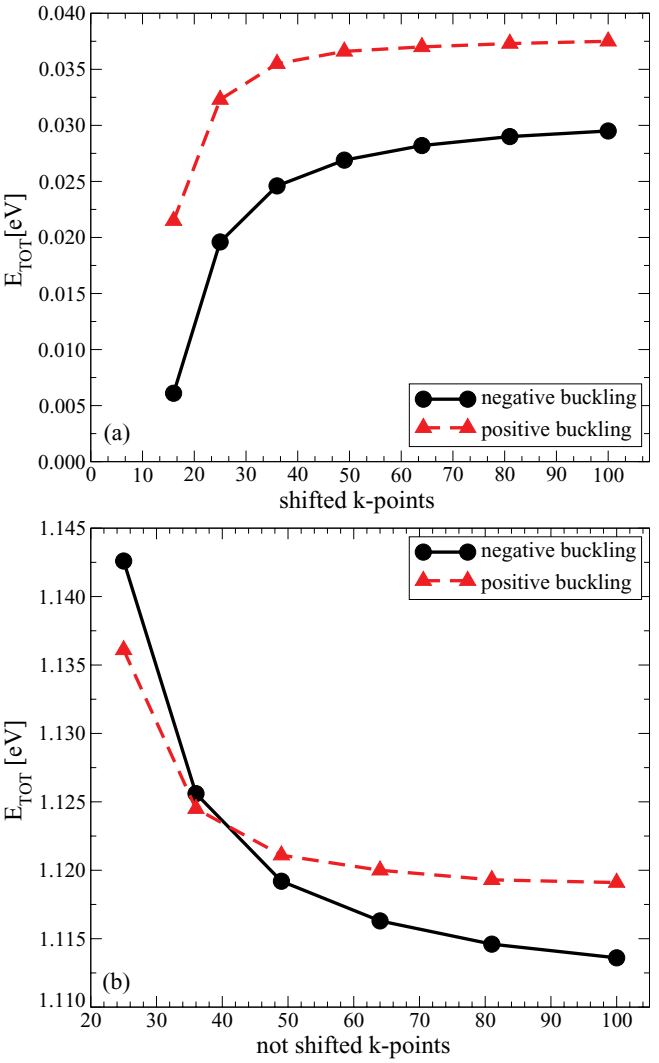

FIG. 5. (Color online) (a) Total DFT-LDA energy versus the number of shifted k points used to sample the IBZ. (b) Total DFT-LDA energy versus the number of not shifted k points used to sample the IBZ.

using shifted k points (a mesh that does not include any high symmetry point and no k points on the border of the BZ), independently on their number, the negative buckling is always the stable configuration [see Fig. 5(a)]. Hence, the quality of the employed k points affects the results, but just when few k points are used.

Recently, Patterson *et al.*[20] have found that using an hybrid DFT method, the pb is 4 meV/surface atom lower in energy than the nb (but the number of used k points is not specified). We have also performed total energy calculations using a norm-conserving PBE[27] pseudopotential (36 shifted k points in IBZ) and a PBE0[28,29] hybrid functional (16 shifted k points in IBZ), finding the same result obtained within the LDA framework: The nb configuration is slightly lower in energy (a few meV) than the pb. Also with the introduction of an electric field perpendicular to the surface (±0.1 and ±0.2 V/Å) and simulating an n-doped and p-doped Si(111)2×1 surface with the addition (or subtraction) of fractional electrons,[30] the nb isomer is favored by a few meV with respect to the

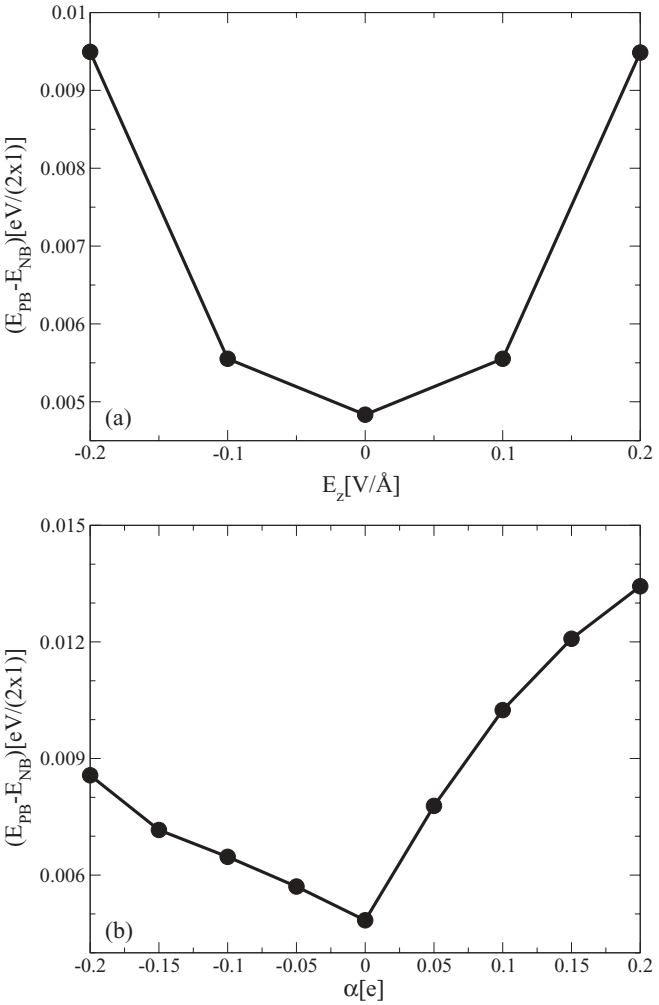

FIG. 6. (a) Energy difference between the two isomers as a function of the strength of an external electric field normal to the surface. (b) Energy difference between the two isomers as a function of excess charge: Injection or subtraction of fractional electrons to simulate n or p doping, respectively.

pb (see Fig. 6). Moreover, we have found out that a higher intensity of the electric field and a higher level of doping (independently of the type) stabilize the negative buckling isomer.

In any case, the energy difference between the two geometric structures is very small, and we can assume that the two isomers are energetically degenerate within the accuracy of the DFT method, as stated in previous works.[3,5,21,26] Thus we would expect that experimentally both isomers coexist but experiments see, most often, the positive buckling configuration. The reason why this happens is not clear. One possibility is that the pb structure is cleavage induced.[31] The inclusion of phonons may also be necessary to explain the STM experimental findings[4] according to which the pb isomer is the stable configuration; anyway we notice that the effect of the zero-point vibrations does not seem to play any role as one can evince from the curvature of the total energy near pb and nb configurations in Fig. 4.

TABLE I. Electronic gaps within DFT-LDA and GW of Si(111)2×1 positive and negative buckling at the surface high symmetry points in IBZ.

Si(111)2×1 Electronic gaps (eV)						
	Positive buckling			Negative buckling		
	$\overline{J}$	$\overline{K}$	$\overline{J'}$	$\overline{J}$	$\overline{K}$	$\overline{J'}$
DFT	0.35	0.62	1.67	0.19	0.35	1.54
GW	0.77	1.03	2.34	0.46	0.63	2.04

B. Electronic properties

The electronic gaps at the surface high-symmetry points, calculated within the density functional theory and within the many-body perturbation theory (GW approximation), are shown in Table I for both isomers.[32]

At the DFT-LDA level we find good agreement with previous results for both isomers.[26,33] At the GW level we find a minimum gap of 0.44 eV near $\frac{\overline{JK}}{2}$ for the Si(111)2×1 negative buckling, while for the positive buckling a GW minimum gap of 0.77 eV is observed near $\overline{J}$. These values are in excellent agreement with the most recent STS experimental results by Bussetti *et al.*[5] For the pb GW band structure we find a good agreement with previous quasiparticle calculations.[22,23] We can observe that the minimum gaps at the surface high symmetry points are larger for the positive buckling isomer: This is indeed true for all the k points along the $\overline{JK}$ direction in reciprocal space, and it will affect the optical properties, as shown in the next section.

In Fig. 7 we show the electronic band structure (empty and filled surface states) for both isomers calculated within the density functional theory (dashed line) and the GW method (solid line) along the $\overline{JK}$ line, which corresponds to the direction perpendicular to the Pandey chains in real space. Two adjacent π chains are about 6.61 Å distant from each other and so their interaction is very weak: This is the reason for the little band dispersion observed along the $\overline{JK}$ direction. On the other hand, the coupling between the orbitals is very strong along each chain, as a direct consequence of the Pandey model, and this is reflected in a marked dispersion of the bands along the lines in reciprocal space corresponding to the π-chain direction.[22]

The maximum value of the filled surface band is at $\overline{J}$ for the positive buckling and between $\frac{\overline{JK}}{2}$ and $\overline{K}$ for the negative buckling; the minimum value of the empty surface band is between $\overline{J}$ and $\frac{\overline{JK}}{2}$ for both isomers. The occupied surface states are located on the upper atoms of the Pandey chains, while the empty states are located on the lower atoms of the π chains: This result comes from the study of the squared modulus of the Kohn-Sham wave functions. For example, we show in Figs. 8 and 9 the squared modulus of the highest occupied surface state and the lowest unoccupied surface state at $\overline{J}$, for both isomers.

We evaluated the impact of the geometry on the electronic properties. The little difference in the buckling amplitudes of the two isomers is not crucial: A slight change in the absolute value of the buckling does not produce sizable changes in the band structure. The important differences concerning the gaps and the dispersion of the two configurations are mainly related

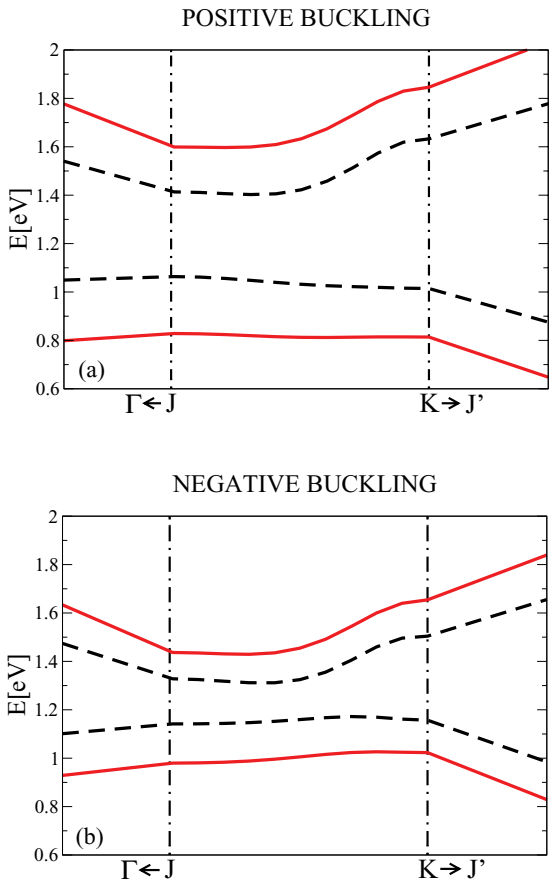

FIG. 7. (Color online) Electronic band structure around the fundamental gap of the Si(111)2×1 positive buckling (a) and negative buckling (b) obtained within DFT-LDA (black dashed lines) and within GW (red solid lines).

to the different sign of the buckling and must be therefore attributed to the interaction between the first and the third atomic layer.

C. Optical properties

The presence of π chains on the Si(111)2×1 surface gives rise to a large anisotropy in the optical properties. This has been proved in 1984 by surface differential reflectivity (SDR) experiments,[34] in which a strong optical response was observed only for light polarized along the Pandey chains (as suggested by Del Sole and Selloni[35]). A previous SDR experiment[36] with unpolarized light, in 1971, had already shown an optical peak at 0.45 eV, connected to a surface exciton, as theoretically described by tight binding[37] and

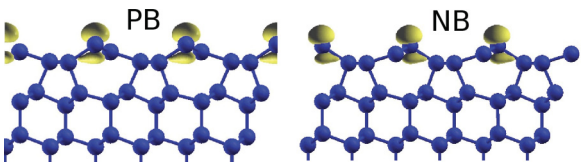

FIG. 8. (Color online) Squared modulus of the Kohn-Sham wave function of the highest occupied surface state at $\overline{J}$ for the Si(111)2×1 positive buckling (left) and negative buckling (right).

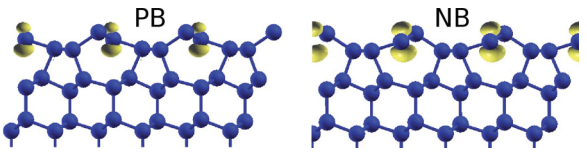

FIG. 9. (Color online) Squared modulus of the Khon-Sham wave function of the lowest unoccupied surface state at $\overline{J}$ for the Si(111)2×1 positive buckling (left) and negative buckling (right).

Bethe-Salpeter[22] calculations. The excitonic peak is also evident in reflectance anisotropy spectroscopy experiments [RAS and SDR results are equivalent[38] in the near-IR region of the Si(111)2×1 spectrum]; a RAS spectrum for Si(111)2×1 surface has been experimentally obtained up to 4.5 eV.[38,39]

The inclusion of the excitonic effects in theoretical simulations of optical spectra has been done by solving the BSE[22,33] and also within TDDFT[33] calculations, but only for the Si(111)2×1 pb. Concerning the Si(111)2×1 nb, only one DFT calculation is, to our knowledge, present in the literature.[20] A calculation of the RAS spectrum with the inclusion of the effects correlated to the electron-hole interaction is still missing.

In order to understand the buckling influence on the surface optical spectra, studies for the nb geometry have been performed in the present work. For the purpose of a direct comparison using the very same convergence criteria (energy cutoff, basis set, pseudopotentials, exchange-correlation functional, k points, and so on), the pb isomer was also investigated. We have obtained the RAS spectra of both isomers of Si(111)2×1 within the density functional theory (in the LDA approximation) and using the GW plus Bethe-Salpeter equation approach.[40]

RAS spectra of positive and negative buckling structures within DFT-LDA, up to 6 eV, are shown in Fig. 10: The RAS spectra of the two isomers differ in shape, intensity, and position of the peak. The Si(111)2×1 negative buckling presents a RAS peak (0.23 eV) at lower energies with respect to the peak of the positive buckling (0.48 eV), and this is related to the differences in the DFT gap values shown in Table I:

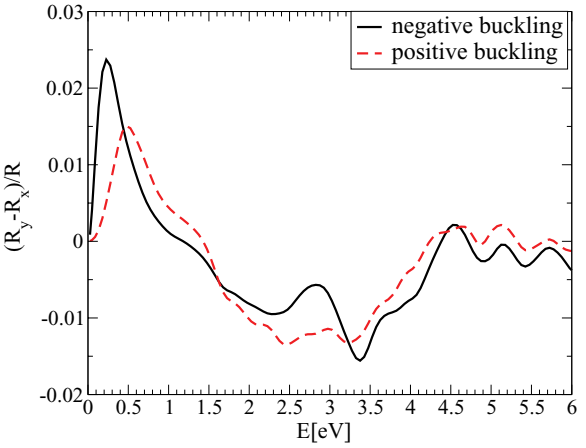

FIG. 10. (Color online) RAS spectra of Si(111)2×1 positive and negative buckling calculated within DFT-LDA. y is the $[1\bar{1}0]$ direction, parallel to the Pandey chains, and x is the $[11\bar{2}]$ direction, perpendicular to the chains.

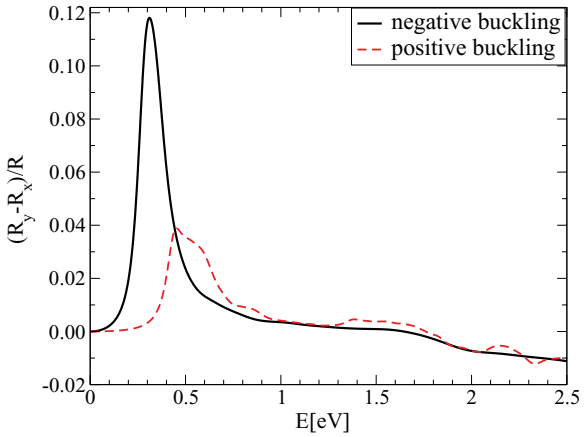

FIG. 11. (Color online) RAS spectra of Si(111)2×1 positive and negative buckling calculated within BSE. y is the $[1\bar{1}0]$ direction, parallel to the Pandey chains, and x is the $[11\bar{2}]$ direction, perpendicular to the chains. An artificial broadening of 0.05 eV has been included.

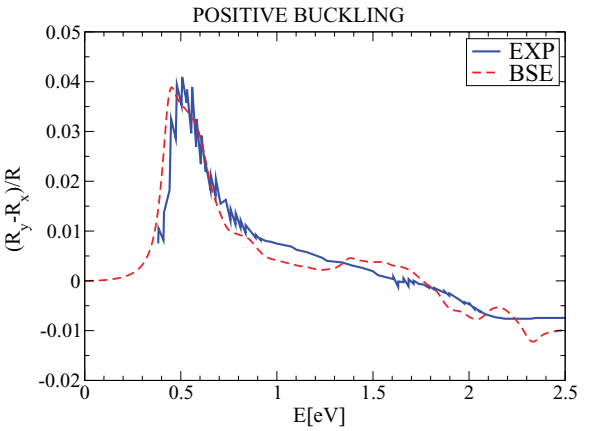

FIG. 12. (Color online) RAS of Si(111)2×1 pb calculated within BSE (red dashed line) compared with experiment[39] (blue solid line). y is the $[1\bar{1}0]$ direction, parallel to the Pandey chains, and x is the $[11\bar{2}]$ direction, perpendicular to the chains.

The electronic gaps of the positive buckling are larger than the electronic gaps of the negative buckling. The RAS peak is more intense for the negative buckling. The intensity ratio between the two isomers is nearly 1.6. The main reasons are related to the different gaps and to the fact that the empty and occupied surface bands of the nb isomer are parallel in a wider BZ region along the $\overline{JK}$ line. This leads to an enhancement of the joint density of states.

The results obtained for the Si(111)2×1 positive buckling are in good agreement with previous DFT-LDA RAS spectra[33]; the redshift of negative buckling RAS peak with respect to the positive buckling was already predicted.[20] Even at the DFT-LDA level we can observe that the optical response of the two isomers is deeply different and so we presume that they can be easily distinguished in RAS experiments. Anyway, in order to compare in a quantitative and qualitative way to the (still missing) experimental data, the introduction of the excitonic effects is necessary.

BSE calculations of both isomers up to 2.5 eV are shown in Fig. 11. The dimension of the excitonic Hamiltonian we have diagonalized is 80 000 × 80 000 in the transition space; more technical details are in Ref. 40. We find the main RAS peak at 0.45 eV for the Si(111)2×1 positive buckling and at 0.31 eV for the Si(111)2×1 negative buckling.

Our results for the positive buckling structure in the IR region are in good agreement with previous BSE calculations[22,33] and with experimental data[34,38,39] as shown in Fig. 12. Thus we can assume the reliability of our results also for what concerns the negative buckling isomer, even if we cannot compare our calculations with an experimental optical spectrum, still missing in literature.

With the inclusion of the excitonic effects, the differences between the spectra of the isomers are even more sizable: The negative buckling shows a narrower and more intense peak at lower energies with respect to the positive buckling. The intensity ratio between the two structures is now nearly 3. As discussed before, one reason for the different optical responses can be traced back from the electronic properties (band structure). Actually, as can be seen in Fig. 13, along the $\overline{JK}$ line the momentum operator matrix elements are nearly the same for the two isomers. The difference in dispersion of the transition energies $E_c(k) - E_v(k)$ is slightly more remarkable since the nb shows a more flat trend. This, together with the smaller gap, seems to be the reason of the larger optical signal in the nb isomer.

The strong anisotropy in surface optical properties, stated in the Pandey model[1] and experimentally well proved,[34] is highlighted in Fig. 14: For both isomers the RAS peak in the IR region is completely related to the optical response along

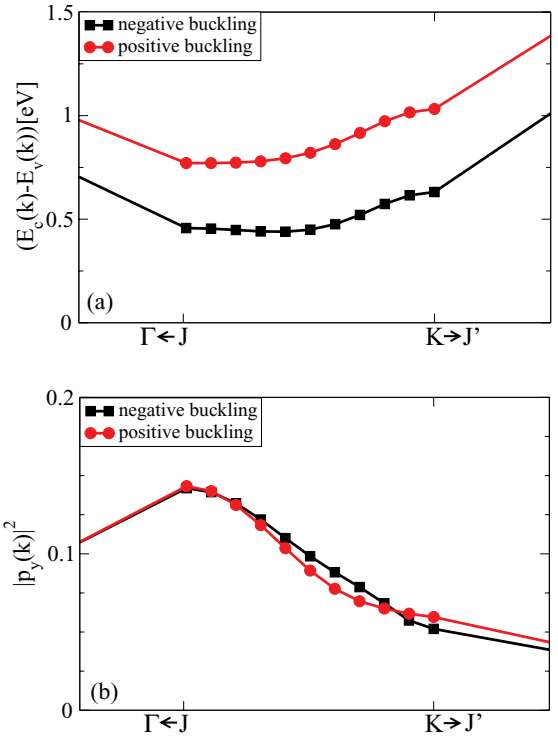

FIG. 13. (Color online) (a) GW energy gaps $E_c(k) - E_v(k)$ for k points along the $\overline{JK}$ line for both isomers. (b) Squared modulus of the momentum operator along the y direction for transitions between the highest occupied and lowest unoccupied surface states along the $\overline{JK}$ line for both isomers of Si(111)2×1.

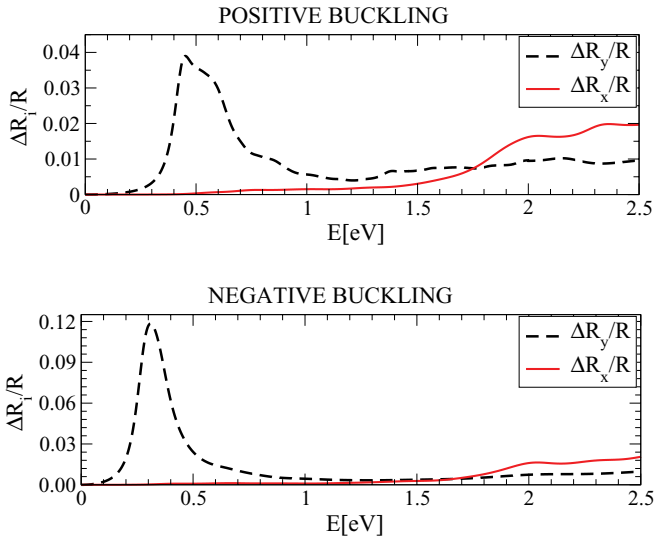

FIG. 14. (Color online) Surface contribution to reflectance for light polarized along x ($[11\bar{2}]$ direction, perpendicular to the π chains) and y ($[1\bar{1}0]$ direction, parallel to the Pandey chains) calculated within BSE. An artificial broadening of 0.05 eV has been included.

the $[1\bar{1}0]$ direction, that is the direction parallel to the Pandey chains (y).

Concerning the surface exciton binding energy E^b we find $E^b = 0.32$ eV for the positive buckling isomer (in good agreement with previous results[22,33,37]) and $E^b = 0.13$ eV for the negative buckling structure. The smaller binding energy for the nb is consistent with a narrower electronic gap and a consequence of a more effective screening. In fact, we find that the "surface" dielectric constant for the nb is about 5 times larger than the one of the pb.

For both isomers, several excitonic eigenvalues can be found below the GW electronic gap but the optical peak is dominated by the lowest energy surface exciton, on which we focus. The other excitons are responsible for the asymmetry of the RAS peak, more evident in the positive buckling isomer that presents a larger number of excitonic states below the GW gap. In order to study the lowest energy excitons we follow Rohlfing and Louie[22]: We consider the hole placed on one of the upper atoms of the Pandey chain (on which we have the maximum distribution of the highest occupied surface state, as shown in Fig. 8 for the $\overline{J}$ point) and we analyze the probability distribution to find the excited electron in real ($|\psi_{\rm exc}(r_e,r_h)|^2$) and reciprocal ($|A_{cv}(k)|^2$) space, where

$$\psi_{\rm exc}(\mathbf{r_e},\mathbf{r_h}) = \sum_{cvk} A_{cv}(k)\phi^*_{vk}(\mathbf{r_h})\phi_{ck}(\mathbf{r_e})$$

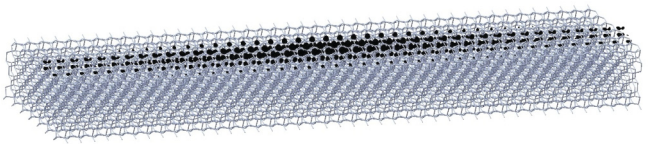

FIG. 15. (Color online) Si(111)2×1 positive buckling. Probability distribution to find the excited electron with the hole fixed on one of the upper atoms of the Pandey chain.

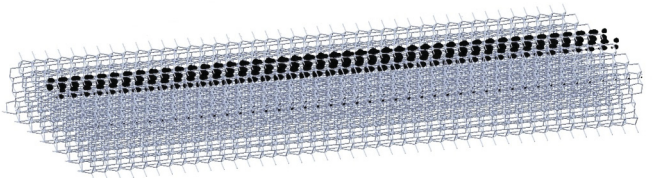

FIG. 16. (Color online) Si(111)2×1 negative buckling. Probability distribution to find the excited electron with the hole fixed on one of the upper atoms of the Pandey chain.

holds. Considering the calculated geometric, electronic, and optical properties of the two configurations of Si(111)2×1, we expect a deep spatial anisotropy of the excitons. As we can see in Figs. 15 and 16, this is indeed the case. The exciton is localized on the surface, along the chains, for both isomers, and it is almost one dimensional. The probability to find the excited electron decays to zero in nearly 13 Å towards the bulk; a localization in the $[11\bar{2}]$ direction (perpendicular to the Pandey chains) is also evident, and is a direct consequence of the weak interaction between the chains. The behavior of the excitonic wave function is visibly different in the $[1\bar{1}0]$ direction (along the Pandey chains): The probability to find the excited electron ranges over a larger distance, decaying to nearly zero in 80 Å in $[1\bar{1}0]$ direction for the positive buckling but remaining still large for the negative buckling. We could just estimate, for the nb, that the excitonic radius is larger than 80 Å. The spatial distribution of the excitonic wave function is thus different for the two isomers: The lowest energy exciton of the negative buckling is more delocalized along the π chain containing the hole. This is in agreement with the lower binding energy of the nb exciton with respect to the pb one.

Despite the localization of the electron-hole pairs over only a few Pandey chains in $[11\bar{2}]$ direction and their restrictions to the first atomic layers, important features of the excitons can be interpreted in terms of (strongly anisotropic) Wannier-Mott excitons. The large binding energy is connected to the depletion of the screening due to dimensionality effects.

Studying the probability in reciprocal space, we find that the transitions involved are mainly those between the highest occupied and the lowest unoccupied surface states, along

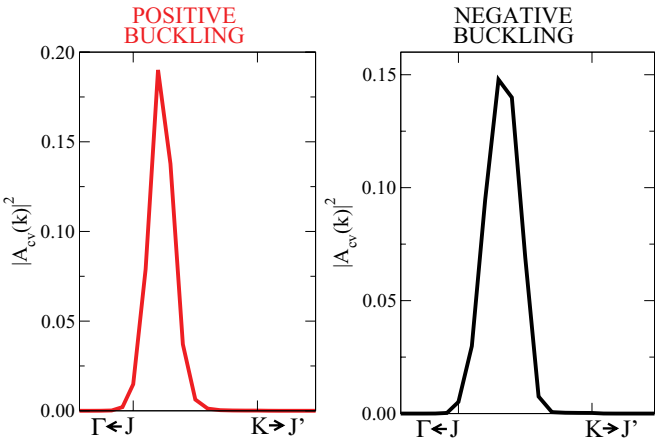

FIG. 17. (Color online) Probability $|A_{cv}(k)|^2$ for transitions between surface states versus k for both isomers of Si(111)2×1.

the $\overline{JK}$ line. We show in Fig. 17 the envelope functions of two representative excitons. Their behavior in k space is in agreement with the electronic properties (the one-dimensional character of the excitons comes from the fact that the band structure is also one dimensional along $\overline{JK}$): For the positive buckling the probability is maximum near $\overline{J}$, at which the minimum GW gap is observed, and it decreases rapidly towards $\overline{K}$; for the negative buckling the maximum probability is near $\frac{\overline{JK}}{2}$, that is where the GW gap is minimum. In Fig. 17 a stronger localization of the negative buckling exciton is evident in the direction perpendicular to the Pandey chains: Again, this can be explained in terms of the more parallel surface bands of the nb isomer [see Fig. 13(a)].

IV. CONCLUSIONS

We have studied the Si(111)2×1 surface using theoretical techniques based on density functional theory and many-body perturbation theory. DFT-LDA results showed that the two Si(111)2×1 isomers, conventionally named positive and negative buckling, are both local stable geometrical configurations, and they are separated by an energetic barrier of less than 0.06 eV/2×1. The slight difference in the geometry of the two isomers, related to the different tilting mode of the topmost atoms of the Pandey chain, produces sizable physical differences in the electronic properties and, consequently, in the optical response. This is a consequence of third-nearest neighbor effects. The most important difference concerns the RAS of the two isomers: The peak of the RAS of the negative buckling is narrower, more intense, and redshifted by about 0.14 eV with respect to the one of the positive buckling. The importance of this observation resides in the possibility to investigate the coexistence of the two configurations at different temperatures and levels of doping, comparing experimental RAS spectra of Si(111)2×1 to the theoretical results obtained in this work. The larger intensity of the negative buckling RAS peak is related to the more parallel empty and occupied surface bands along the $\overline{JK}$ line for negative buckling, and to the narrower electronic gap. The solution of the Bethe-Salpeter equation put in evidence the quasi-one-dimensional character of the exciton responsible for the RAS main peak for both isomers, that is very localized along the direction perpendicular to the Pandey chains, and whose probability distribution is extended over 80 Å along the chains for the positive buckling and even more for the negative buckling. The larger delocalization of the exciton in the negative buckling is at the origin of the small value of its binding energy (∼0.1 eV).

ACKNOWLEDGMENTS

We would like to thank CINECA, CASPUR-MATRIX, and ENEA-CRESCO supercomputer centers for cpu time. We acknowledge financial support within the EU FP7 CLERMONT4 project (GA235114). We also acknowledge ETSF.[41] We dedicate this work to Rodolfo Del Sole.

[1] K. C. Pandey, Phys. Rev. Lett. **47**, 1913 (1981).
[2] J. E. Northrup and M. L. Cohen, Phys. Rev. Lett. **49**, 1349 (1982).
[3] F. Ancilotto, W. Andreoni, A. Selloni, R. Car, and M. Parrinello, Phys. Rev. Lett. **65**, 3148 (1990).
[4] S. Nie, R. M. Feenstra, J. Y. Lee, and M. H. Kang, J. Vac. Sci. Technol. A **22**, 1671 (2004).
[5] G. Bussetti, B. Bonanni, S. Cirilli, A. Violante, M. Russo, C. Goletti, P. Chiaradia, O. Pulci, M. Palummo, R. Del Sole, P. Gargiani, M. G. Betti, C. Mariani, R. M. Feenstra, G. Meyer, and K. H. Rieder, Phys. Rev. Lett. **106**, 067601 (2011).
[6] R. M. Feenstra, G. Bussetti, B. Bonanni, A. Violante, C. Goletti, P. Chiaradia, M. G. Betti, and C. Mariani, J. Phys.: Condens. Matter **24**, 354009 (2012).
[7] K. Löser, M. Wenderoth, T. K. A. Spaeth, J. K. Garleff, R. G. Ulbrich, M. Pötter, and M. Rohlfing, Phys. Rev. B **86**, 085303 (2012).
[8] M. Rohlfing, M. Palummo, G. Onida, and R. Del Sole, Phys. Rev. Lett. **85**, 5440 (2000).
[9] P. H. Hahn, W. G. Schmidt, F. Bechstedt, O. Pulci, and R. Del Sole, Phys. Rev. B **68**, 033311 (2003).
[10] http://www.quantum-espresso.org/.
[11] D. M. Ceperley and B. J. Alder, Phys. Rev. Lett. **45**, 566 (1980).
[12] J. P. Perdew and A. Zunger, Phys. Rev. B **23**, 5048 (1981).
[13] H. J. Monkhorst and J. D. Pack, Phys. Rev. B **13**, 5188 (1976).
[14] For a review, see for example, F. Aryasetiawan and O. Gunnarsson, Rep. Prog. Phys. **61**, 237 (1998).
[15] E. E. Salpeter and H. A. Bethe, Phys. Rev. **84**, 1232 (1951).
[16] EXC code http://theory.polytechnique.fr/codes/exc/.
[17] D. E. Aspnes, J. F. Harbinson, A. A. Studna, and L. T. Florez, J. Vac. Sci. Technol. A **6**, 1327 (1988).
[18] P. Weightman, D. S. Martin, R. J. Cole, and T. Farrel, Rep. Prog Phys. **68**, 1251 (2005).
[19] F. Manghi, E. Molinari, R. Del Sole, and A. Selloni, Phys. Rev. B **39**, 13005 (1989).
[20] C. H. Patterson, S. Banerjee, and J. F. McGilp, Phys. Rev. B **84**, 155314 (2011).
[21] F. Bechstedt, A. A. Stekolnikov, J. Furthmüller, and P. Käckell, Phys. Rev. Lett. **87**, 016103 (2001).
[22] M. Rohlfing and S. G. Louie, Phys. Rev. Lett. **83**, 856 (1999).
[23] J. E. Northrup, M. S. Hybertsen, and S. G. Louie, Phys. Rev. Lett. **66**, 500 (1991).
[24] F. Bechstedt, *Principles of Surface Physics* (Springer, Berlin, 2003).
[25] G. Xu, B. Deng, Z. Yu, S. Y. Tong, M. A. Van Hove, F. Jona, and I. Zasada, Phys. Rev. B **70**, 045307 (2004).
[26] M. Zitzlsperger, R. Honke, P. Pavone, and U. Schröder, Surf. Sci. **377–379**, 108 (1997).
[27] J. P. Perdew, K. Burke, and M. Ernzerhof, Phys. Rev. Lett. **77**, 3865 (1996).
[28] J. P. Perdew, M. Ernzerhof, and K. Burke, J. Chem. Phys. **105**, 9982 (1996).
[29] C. Adamo and V. Barone, J. Chem. Phys. **110**, 6158 (1999).
[30] K. Seino, W. G. Schmidt, and F. Bechstedt, Phys. Rev. Lett. **93**, 036101 (2004).
[31] D. Reichardt, Prog. Surf. Sci. **35**, 63 (1990).

[32]Our GW calculations are performed at the G_0W_0 level. The screening has been calculated using 231 q points in IBZ, 1977 plane waves, and 452 empty bands; for Σ_x calculation we have employed 4979 plane waves, while for Σ_c calculation 1977 plane waves and 452 empty bands have been used.

[33]O. Pulci, A. Marini, M. Palummo, and R. Del Sole, Phys. Rev. B **82**, 205319 (2010).

[34]P. Chiaradia, A. Cricenti, S. Selci, and G. Chiarotti, Phys. Rev. Lett. **52**, 1145 (1984).

[35]R. Del Sole and A. Selloni, Phys. Rev. B **30**, 883 (1984).

[36]G. Chiarotti, S. Nannarone, R. Pastore, and P. Chiaradia, Phys. Rev. B **4**, 3398 (1971).

[37]L. Reining and R. Del Sole, Phys. Rev. Lett. **67**, 3816 (1991).

[38]C. Goletti, G. Bussetti, F. Arciprete, P. Chiaradia, and G. Chiarotti, Phys. Rev. B **66**, 153307 (2002).

[39]C. Goletti, G. Bussetti, P. Chiaradia, and G. Chiarotti, J. Phys.: Condens. Matter **16**, S4289 (2004).

[40]For BSE calculations we have used 800 k points in the Brillouin zone (231 in IBZ), 3003 plane waves for the wave functions, 503 G vectors for the local fields, 10 conduction, and 10 valence states.

[41]A. Y. Matsuura, N. Thrupp, X. Gonze, Y. Pouillon, G. Bruant, and G. Onida, Comput. Sci. Eng. **14**, 22 (2012).